

Unsupervised Learning for Passive Beamforming

Jiabao Gao, Caijun Zhong, Xiaoming Chen, Hai Lin and Zhaoyang Zhang

Abstract—Reconfigurable intelligent surface (RIS) has recently emerged as a promising candidate to improve the energy and spectral efficiency of wireless communication systems. However, the unit modulus constraint on the phase shift of reflecting elements makes the design of optimal passive beamforming solution a challenging issue. The conventional approach is to find a suboptimal solution using the semi-definite relaxation (SDR) technique, yet the resultant suboptimal iterative algorithm usually incurs high complexity, hence is not amenable for real-time implementation. Motivated by this, we propose a deep learning approach for passive beamforming design in RIS-assisted systems. In particular, a customized deep neural network is trained offline using the unsupervised learning mechanism, which is able to make real-time prediction when deployed online. Simulation results show that the proposed approach significantly outperforms the conventional SDR-based method in terms of both performance and complexity.

Index Terms—Reconfigurable intelligent surface, passive beamforming, deep learning, unsupervised learning

I. INTRODUCTION

With the commercialization of fifth generation wireless communication systems, how to reduce the network deployment cost and energy consumption has stood out as one of the major challenges for future sustainable and green wireless systems. Recently, the reconfigurable intelligent surface (RIS) has emerged as a promising candidate to tackle the above challenges thanks to low manufacturing, hardware and energy cost.¹ Specifically, the RIS is a planar array composed of a large number of low-cost reconfigurable reflecting elements, which are able to modify the phase shift of the incident signal. Through proper adjustment of the phase shifts, the reflected signal from the RIS can add coherently with the signal from the direct path at the intended user to substantially improve the receive signal strength.

It is worth noting that RIS is a brand new technology that significantly differs from other related technologies such as amplify-and-forward (AF) relaying and backscatter communications. For instance, compared to AF relaying, the RIS does not need to generate its own transmission signal, but passively reflects the incident signal, hence having much lower power consumption. Compared to the backscatter communications, the RIS does not deliver any of its own information, but only acts as a helper to enhance the performance of existing links [1].

Apparently, the design of phase shifts, also known as passive beamforming, is of critical importance for RIS-assisted communication systems. However, the non-convexity introduced by unit modulus constraint makes the derivation of optimal solution difficult. In [1], a suboptimal solution for passive beamforming in RIS-assisted single user multiple-input single-output downlink systems is proposed using the

conventional semi-definite relaxation (SDR) technique. However, the SDR-based approach is computationally expensive and is not amenable for real-time implementation. In [3], the authors investigated the multi-user scenario and addressed the problem of maximizing the achievable rate by combining alternating maximization with the majorization-minimization method. Later on, by imposing a rank-1 constraint on the channel between the source and RIS, a closed-form analytical solution was derived in [5]. Besides, energy efficiency for RIS-assisted systems was investigated in [6], while [7] tackled the problem of minimizing the total transmit power subject to individual signal-to-interference-plus-noise ratio constraint. In practice, discrete phase shifts are used due to hardware constraint. In this regard, [8] and [9] have investigated performance of RIS systems with only a finite number of phase shift levels.

In the past few years, deep learning (DL) has demonstrated its remarkable potential in dealing with non-convex problems [10, 11]. In addition, DL based approach enables fast computation compared with the traditional iterative algorithms [12]. These desirable features make it appealing for many practical applications in wireless communications [13]. In the context of RIS-assisted wireless communications, a supervised learning based approach was proposed in [14] where a deep neural network (DNN) is trained offline to establish the implicit relationship between the measured coordinate information and RIS's phase configuration. Nevertheless, a major issue for supervised learning is how to obtain labels. In [14], the optimal labels were obtained via exhaustive search, which is extremely expensive to implement in practice, especially if large number of training samples are required.

To overcome the drawbacks of supervised learning, a promising candidate is the unsupervised learning based method, where no labels are required [10, 15]. Also, unlike the supervised learning approach, whose performance is constrained by the achievable performance of the algorithm producing the training labels, the performance of unsupervised learning mechanism is no longer constrained since the trained DNN explores new knowledge rather than simply mimicking the baseline algorithm. Motivated by these important observations, we propose to adopt the unsupervised learning mechanism for passive beamforming design. In particular, a customized DNN architecture is developed for the passive beamforming design problem, and a set of tailored features are selected for the training process. Simulation results show that the proposed unsupervised learning based approach not only achieves superior performance, but also requires much less computational time when compared with the conventional SDR-based approach.

The rest of this paper is organized as follows. Section II introduces the RIS-assisted wireless communication system model and the problem formulation of passive beamforming. In Section III, conventional approaches for the passive beam-

¹Please note, there have been other terminologies for RIS, such as intelligent reflecting surface [1], intelligent wall [2], passive intelligent mirror [3], and reconfigurable metasurface [4].

forming problem in single antenna case and multi-antenna case are briefly introduced. The unsupervised learning based approach is proposed in Section IV, and Section V presents simulation results to evaluate the performance of the proposed approach. Finally, the paper is concluded in Section VI.

Notations: Scalars, vectors and matrices are denoted by italic letters, bold-face lower-case and bold-face upper-case letters, respectively. $\mathbb{C}^{x \times y}$ denotes the space of $x \times y$ complex vectors or matrices. $\|\cdot\|$ denotes the Euclidean norm and $\text{diag}(\cdot)$ denotes the diagonalization of a vector. Superscript $*$, T and H denote conjugate, transpose and conjugate transpose respectively. $\text{tr}(\cdot)$ denotes the trace of a matrix and $\mathbf{X} \succeq 0$ means that \mathbf{X} is positive-semidefinite. $\text{Norm}(\cdot)$ is the operation of normalizing a complex scalar's modulus, and $\mathbf{x}[1:N]$ fetches the first N elements of vector \mathbf{x} . $\mathcal{CN}(\mu, \sigma^2)$ denotes the distribution of a circularly symmetric complex Gaussian random variable with mean μ and covariance σ^2 .

II. SYSTEM MODEL AND PROBLEM FORMULATION

We consider a three-node system consisting of an access point (AP) equipped with M antennas, a RIS equipped with N reflecting elements and a single antenna user as illustrated in Fig. 1. A controller connecting the AP and RIS is used to adaptively adjust the phase shifts of reflecting elements and coordinate the switching between the receiving mode for channel estimation and the reflecting mode for signal reflection [2]. The baseband receive signal at the user is the superposition of the direct signal from the AP and the reflected signal from RIS, which can be expressed as

$$y = (\mathbf{G}\Theta\mathbf{h}_r + \mathbf{h}_d)^T \mathbf{w}s + n, \quad (1)$$

where $\mathbf{w} \in \mathbb{C}^{M \times 1}$ denotes the transmit beamforming vector satisfying $\|\mathbf{w}\|^2 \leq p$, and s is the information symbol with unit power drawn from a certain constellation set. Also, $\mathbf{h}_d \in \mathbb{C}^{M \times 1}$, $\mathbf{h}_r \in \mathbb{C}^{N \times 1}$ and $\mathbf{G} \in \mathbb{C}^{M \times N}$ denotes the channels of the direct link between AP and user, the reflecting link between RIS and user, and the link between RIS and AP, respectively. All the channels are assumed to be quasi-static and flat-fading. In practice, the channel state information can be obtained by different methods as pointed out in [16]. Moreover, $\Theta = \text{diag}\{\boldsymbol{\theta}\}$ is the phase shift matrix of the RIS, where $\boldsymbol{\theta} = [\theta_1, \theta_2, \dots, \theta_N]^T \in \mathbb{C}^{N \times 1}$ and $|\theta_n| = 1$. The additive noise $n \sim \mathcal{CN}(0, \sigma^2)$. The signals reflected by the RIS for two or more times are ignored due to severe path loss [1]. Therefore, the receive SNR γ at the user can be expressed as

$$\gamma = \frac{1}{\sigma^2} |(\mathbf{G}\Theta\mathbf{h}_r + \mathbf{h}_d)^T \mathbf{w}|^2. \quad (2)$$

Given Θ , it is well known that maximum-ratio transmission (MRT) is the optimal transmit beamforming strategy [17], i.e., $\mathbf{w}_{\text{opt}}^T = \sqrt{p} \frac{(\mathbf{G}\Theta\mathbf{h}_r + \mathbf{h}_d)^H}{\|\mathbf{G}\Theta\mathbf{h}_r + \mathbf{h}_d\|}$. Substituting \mathbf{w}_{opt} into Equation (2), the optimal phase shift $\boldsymbol{\theta}$ at the RIS maximizing the transmission rate is the solution of the following optimization problem

$$\text{P1:} \quad \max_{\boldsymbol{\theta}} \quad \|\mathbf{G}\Theta\mathbf{h}_r + \mathbf{h}_d\|^2 \quad (3)$$

$$\text{s.t.} \quad |\theta_n| = 1, \quad n = 1, \dots, N. \quad (4)$$

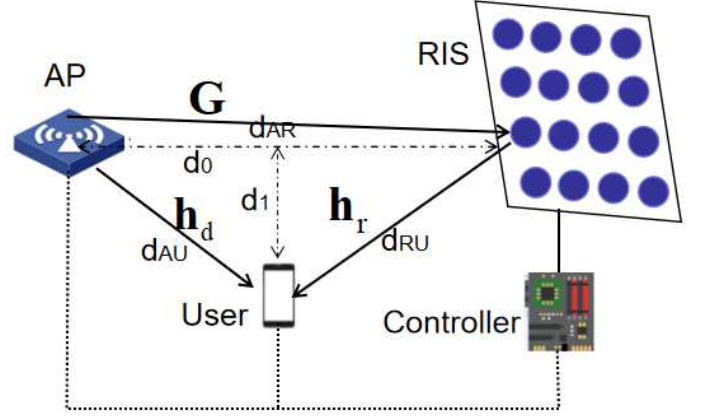


Fig. 1. System model.

III. CONVENTIONAL APPROACH

Problem P1 is a typical non-convex quadratically constrained quadratic program (QCQP), hence the optimal solution is intractable except for the single antenna case. For $M \geq 2$, the common approach is to find a suboptimal solution using techniques such as SDR.

A. Single antenna case

When $M = 1$, problem P1 can be rewritten as

$$\text{P2:} \quad \max_{\boldsymbol{\theta}} \quad |r|^2 \quad (5)$$

$$\text{s.t.} \quad |\theta_n| = 1, \quad n = 1, \dots, N, \quad (6)$$

where $r \triangleq \sum_{n=1}^N g_n h_{r_n} \theta_n + h_d$. It is easy to show that the maximum can be achieved by aligning the phases of $g_n h_{r_n} \theta_n$ to that of h_d . Hence, the optimal phase shift θ_n can be computed as

$$\theta_n^{\text{opt}} = \text{Norm} \left(\frac{h_d}{g_n h_{r_n}} \right), \quad (7)$$

B. Multi-antenna case

We now consider the multi-antenna case, i.e., $M \geq 2$. According to [1], problem P1 can be reformulated as the following homogeneous QCQP

$$\text{P3:} \quad \max_{\bar{\boldsymbol{\theta}}} \quad \bar{\boldsymbol{\theta}}^H \mathbf{R} \bar{\boldsymbol{\theta}} \quad (8)$$

$$\text{s.t.} \quad |\theta_n| = 1, \quad n = 1, \dots, N, \quad (9)$$

where

$$\bar{\boldsymbol{\theta}} = \begin{bmatrix} \boldsymbol{\theta} \\ t \end{bmatrix}, \quad \mathbf{R} = \begin{bmatrix} \mathbf{D}_h^H \mathbf{G}^H \mathbf{G} \mathbf{D}_h & \mathbf{D}_h^H \mathbf{G}^H \mathbf{h}_d \\ \mathbf{h}_d^H \mathbf{G} \mathbf{D}_h & 0 \end{bmatrix},$$

$\mathbf{D}_h = \text{diag}\{\mathbf{h}_r\}$, and t is an auxiliary variable.

Define $\mathbf{Q} \triangleq \bar{\boldsymbol{\theta}} \bar{\boldsymbol{\theta}}^H$, we have $\bar{\boldsymbol{\theta}}^H \mathbf{R} \bar{\boldsymbol{\theta}} = \text{tr}(\mathbf{R} \mathbf{Q})$. \mathbf{Q} is a positive-semidefinite matrix with rank one. By relaxing the rank-one constraint, P3 can be converted to the following convex problem

$$\text{P4:} \quad \max_{\mathbf{Q}} \quad \text{tr}(\mathbf{R} \mathbf{Q}) \quad (10)$$

$$\text{s.t.} \quad \mathbf{Q} \succeq 0; \quad \mathbf{Q}_{n,n} = 1, \quad n = 1, \dots, N+1. \quad (11)$$

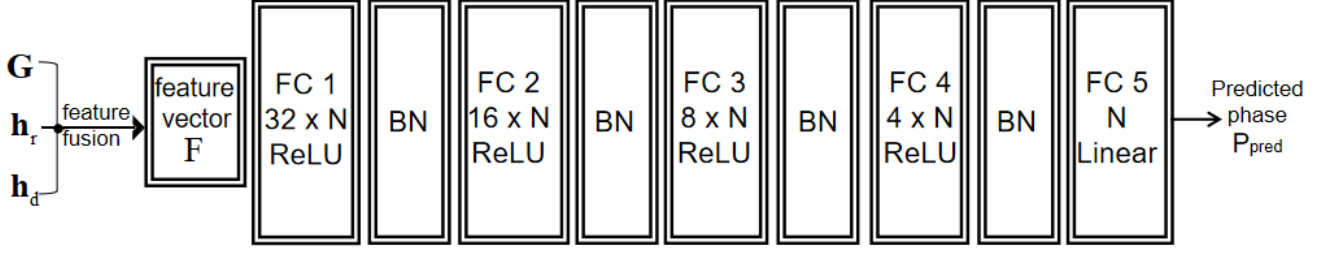


Fig. 2. Network architecture.

From the optimal solution of P4, a suboptimal solution of P3 can be obtained through the technique of randomization. Then, the suboptimal solution of P1 can be obtained as $\theta = \text{Norm}(\bar{\theta}[1 : N] / \bar{\theta}_{N+1})$.

IV. UNSUPERVISED LEARNING BASED APPROACH

The performance of suboptimal solutions obtained by conventional optimization based approaches can not be guaranteed, and they in general incur high complexity. Motivated by these issues, we propose a DL based framework to tackle problem P1.

A. Feature Design

From Equation (3), it is intuitive to use the channels \mathbf{G} , \mathbf{h}_r and \mathbf{h}_d as the input. However, such a simple approach turns out to be ineffective and problematic.

To see this, let us define $\mathbf{r} \triangleq \mathbf{G}\Theta\mathbf{h}_r + \mathbf{h}_d$, then the i -th element of \mathbf{r} can be written as

$$r_i = \sum_{n=1}^N g_{i,n} h_{r,n} \theta_n + h_{d,i}, \quad i = 1, \dots, M, \quad (12)$$

which explicitly shows the product structure of \mathbf{G} and \mathbf{h}_r . Hence, instead of simply choosing \mathbf{G} , \mathbf{h}_r , a more appropriate feature is to use the product of the elements of \mathbf{G} and \mathbf{h}_r . In addition, the real and imaginary parts are treated as separate features. As such, the final feature vector is denoted by $\mathbf{F} \in \mathbb{C}^{2(NM+M) \times 1}$. It is worth pointing out that the above feature design not only reduces the dimension of input, but also exploits the inherent structural information, therefore substantially improves the training efficiency and network performance.

B. Loss Function

The loss function is defined as

$$\text{Loss} = -\frac{1}{K} \sum_{k=1}^K \|\mathbf{G}^k \Theta^k \mathbf{h}_r^k + \mathbf{h}_d^k\|^2, \quad (13)$$

where K is the number of training samples in a mini batch. Please note, unlike the commonly used mean square error in supervised learning systems, the loss function is set to be the negative of the objective function in P1, which reflects the unsupervised nature of the proposed approach. Besides, the following Lambda layer is implemented to convert the predicted real phase shift vector \mathbf{p}_{pred} to its complex form θ_{pred} for loss computation [10]

$$\theta_{pred} = e^{j \cdot \mathbf{p}_{pred}} = \cos(\mathbf{p}_{pred}) + j \cdot \sin(\mathbf{p}_{pred}). \quad (14)$$

C. Network Architecture and training

Fig. 2 illustrates the adopted architecture of the neural network, which is termed as “RISBFNN”. In particular, RISBFNN is made up of 5 fully-connected (FC) layers with $32N$, $16N$, $8N$, $4N$ and N neurons respectively. The idea of setting the number of neurons being proportional to N is to ensure adequate learning ability when the system scales. For activation function, the first four FC layers adopt the rectified linear unit (ReLU), while FC5 uses a Linear unit to output the phase shift prediction.

To train the network, adam optimizer with initial learning rate 0.001 is used. Also, the number of maximal epoch is set to 1000, and early stopping with patience 20 is applied to improve the training efficiency. In addition, to expedite the convergence, the learning rate decays by a factor of 0.33 whenever the validation loss does not decrease for a consecutive 10 epochs.

During network training, it turns out that Batch Normalization (BN) layer [18] and batch size are two key hyperparameters to make RISBFNN work effectively. An exemplary training process is illustrated in Fig. 3 where $M = 8, N = 64$. As can be readily observed, without BN layer and sufficiently large batch size, both the training and validation loss cannot decrease. Through extensive experiments, we found that a BN layer after each FC layer and a batch size of 5000 work well under various settings.

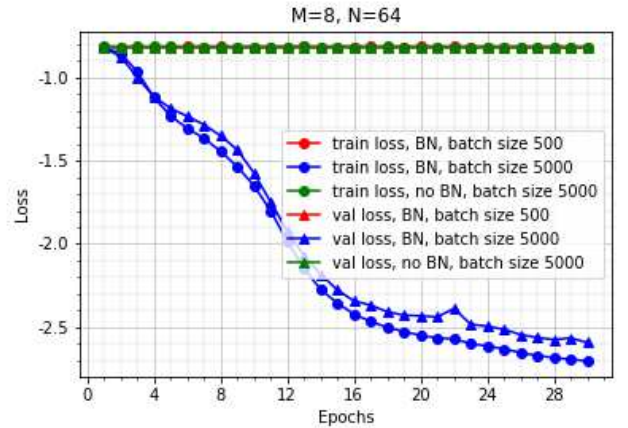


Fig. 3. Impact of BN and batch size on loss.

The impact of the number of training samples is illustrated in Fig. 4. As can be observed, the performance settles when the number of training samples is sufficiently large. If the number

of training samples is small, then overfitting occurs which substantially degrades the system performance. In addition, the minimum required sample number is configuration dependent, for instance, when $M = 4, N = 8$, 150000 samples are sufficient, while for the case $M = 4, N = 32$, 350000 samples are required. It is also worth highlighting that, since unsupervised learning is adopted, no labels are required, which significantly reduces the cost of obtaining training samples.

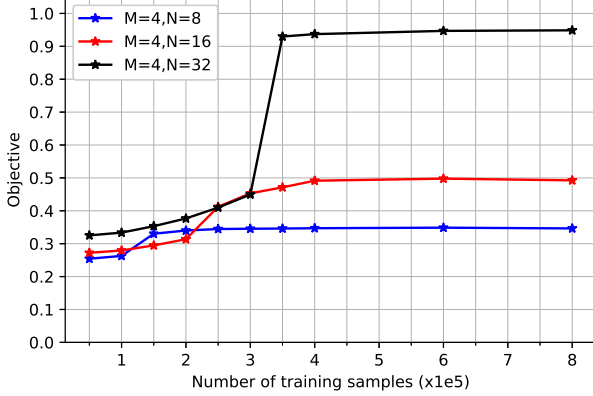


Fig. 4. Impact of the number of training samples.

Taking training efficiency, testing performance and stability into consideration, we generate 800000, 200000 and 10000 samples for training, validation and testing respectively. It is also worth mentioning that, prior to training, standardization preprocessing is performed on each dimension of features by subtracting its average and dividing its standard deviation. All the training is executed by a GeForce GTX 1080 Ti GPU.

V. SIMULATION RESULTS

In this section, simulation results are provided to demonstrate the performance of the proposed unsupervised learning approach.² We consider a similar indoor scenario as [14], where all the channels are modeled by independent Rayleigh small-scale fading, and the path loss in dB is computed as $20.4 \log_{10}(d/d_{\text{ref}})$ [19], with d being the distance between transmitter and receiver in meters and $d_{\text{ref}} = 1\text{m}$ denoting the reference distance. As illustrated in Fig. 1, the distance from AP to RIS is denoted by d_{AR} , while the distance from AP to user and from RIS to user can be computed as $d_{\text{AU}} = \sqrt{d_0^2 + d_1^2}$ and $d_{\text{RU}} = \sqrt{(d_{\text{AR}} - d_0)^2 + d_1^2}$ respectively, where d_1 is the vertical distance from user to the horizontal connection line of AP and RIS while d_0 is the distance from AP to the intersection. For the simulations, d_{AR} is set to be 8m, while d_0 and d_1 follows uniform distribution with range $[0, 8]$ and $[1, 6]$ respectively.

A. Impact of N

Fig. 5 illustrates the impact of the number of reflecting elements N on the performance. As can be readily observed, the performance of both the RISBFNN and SDR approaches

improve as N becomes larger. This is intuitive, since increasing N can enhance the effective gain of the reflecting path. Also, for the single antenna case, the two curves almost overlap, which indicates that the proposed RISBFNN can achieve near optimal performance. In addition, for the multi-antenna case, the proposed RISBFNN significantly outperforms the SDR approach, especially in the large N regime. Interestingly, for the SDR approach, increasing the antenna number does not necessarily provide performance gain compared with the single antenna case. As shown in Fig. 5, with 8 antennas, the performance becomes inferior to that of single antenna case when $N \geq 40$. This is mainly due to the inherent suboptimality of the SDR approach. In contrast, the performance of the RISBFNN improves consistently with the increase of antenna number, thereby manifesting the superiority of the proposed unsupervised learning strategy.

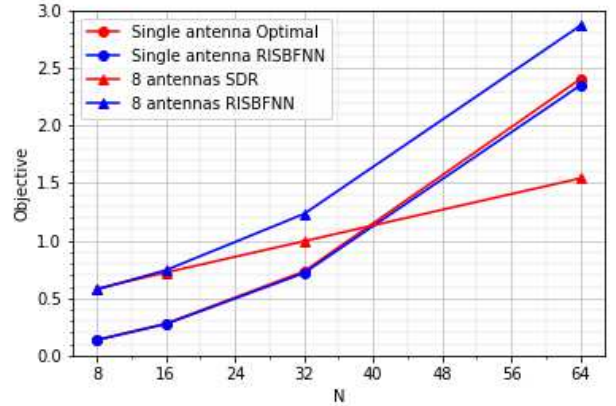


Fig. 5. Impact of the number of reflecting elements N .

B. Impact of M

Fig. 6 depicts the impact of M on the performance. Once again, we see that the performance of both the RISBFNN and SDR approaches improve as the number of antennas increases. However, unlike the RISBFNN approach, increasing M does not guarantee performance enhancement for the SDR approach. For instance, with $N = 32$, the achievable performance when $M = 2, \dots, 5$ is actually inferior to that of the single antenna scenario. In addition, the proposed RISBFNN approach always outperform the SDR approach, and the performance gap is more significant when N is large. Nevertheless, the performance gap gradually narrows down when M increases. In general, the advantage of RISBFNN is most substantial in the case with few antennas and many reflecting elements, a scenario that is practically appealing since installing more reflecting elements is much cheaper than using extra radio-frequency chains.

C. Computation Complexity

Table I compares the average running time consumed by RISBFNN and SDR under various system setups. For a fair comparison, both algorithms are executed on the same Intel i7-8700 CPU. P4 is solved by the popular convex optimization

²For reproducible research, all source codes can be found at <https://github.com/EricGJB/UN-Based-RISBF>

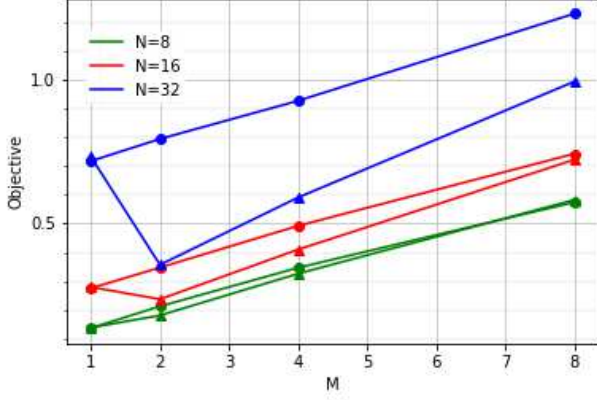


Fig. 6. Impact of antenna number M on the performance. Curves marked with circles and triangles represent the RIS-BFNN and baseline methods (optimal solution in Equation (7) when $M = 1$ and SDR approach when $M \geq 2$) respectively.

solver CVX [20]. As we can see, the RISBFNN runs thousands of times faster than the SDR approach, which makes it a potential candidate for real-time configuration of phase shifts in large scale RIS-assisted systems.

| Algorithm Parameters | RISBFNN (ms) | SDR (ms) |
|-------------------------|--------------|----------|
| $M = 2, N = 16$ | 0.0399 | 199.2 |
| $M = 4, N = 32$ | 0.0487 | 287.7 |
| $M = 8, N = 64$ | 0.1167 | 715.3 |

TABLE I. Average time consumption of two algorithms.

VI. CONCLUSION

In this letter, we have developed an unsupervised learning based approach for passive beamforming in RIS-assisted communication systems. Through extensive simulations, it has been demonstrated that the proposed approach is capable of performing real-time phase shift configuration. Moreover, it substantially outperforms the traditional SDR-based optimization algorithms, with much less computational overhead. In the future, we will consider to extend the proposed framework to more challenging multiuser case. Besides, the use of advanced learning approaches like multi-modal DL [21] to improve system performance is also a research direction worth investigating.

REFERENCES

- [1] Q. Wu and R. Zhang, "Intelligent reflecting surface enhanced wireless network: Joint active and passive beamforming design," in *Proc. IEEE GLOBECOM*, Dec. 2018.
- [2] L. Subrt and P. Pechac, "Intelligent walls as autonomous parts of smart indoor environments," *IET communications*, vol. 6, no. 8, pp. 1004-1010, May 2012.
- [3] C. Huang, *et al.*, "Achievable rate maximization by passive intelligent mirrors," in *Proc. IEEE ICASSP*, 2018.
- [4] M. Di Renzo, *et al.*, "Smart radio environments empowered by AI reconfigurable meta-surfaces: An idea whose time has come," *EURASIP J. Wireless Commun. Netw.*, vol. 2019:129, May. 2019.
- [5] P. Wang, *et al.*, "Intelligent reflecting surface-assisted millimeter wave communications: Joint active and passive precoding design," 2019, [Online]. Available: <https://arxiv.org/abs/1908.10734>.
- [6] C. Huang, *et al.*, "Reconfigurable intelligent surfaces for energy efficiency in wireless communication," *IEEE Trans. Wireless Commun.*, vol. 18, no. 8, pp. 4157-4170, 2019.
- [7] Q. Wu and R. Zhang, "Intelligent reflecting surface enhanced wireless network via joint active and passive beamforming," *IEEE Trans. Wireless Commun.*, DOI:10.1109/TWC.2019.2936025, Aug. 2019.
- [8] Q. Wu and R. Zhang, "Beamforming optimization for wireless network aided by intelligent reflecting surface with discrete phase shifts," 2019, [Online]. Available: <https://arxiv.org/abs/1906.03165>.
- [9] Q. Wu and R. Zhang, "Beamforming optimization for intelligent reflecting surface with discrete phase shifts," in *Proc. IEEE ICASSP*, pp. 7830-7833, 2019.
- [10] T. Lin and Y. Zhu, "Beamforming design for large-scale antenna arrays using deep learning," 2019, [Online]. Available: <https://arxiv.org/abs/1904.03657>.
- [11] G. Aceto, *et al.*, "Mobile encrypted traffic classification using deep learning: Experimental evaluation, lessons learned, and challenges," *IEEE Trans. Netw. Service Manag.*, vol. 16, no. 2, pp. 445-458, June. 2019.
- [12] H. Sun, *et al.*, "Learning to optimize: training deep neural networks for wireless resource management," *IEEE Trans. Signal Process.*, vol. 66, pp. 5438-5453, Oct. 2018.
- [13] A. Zappone, M. D. Renzo and M. Debbah, "Wireless networks design in the era of deep learning: Model-based, AI-based, or both," 2019, [Online]. Available: <https://arxiv.org/abs/1902.02647>.
- [14] C. Huang, *et al.*, "Indoor signal focusing with deep learning designed reconfigurable intelligent surfaces," 2019, [Online]. Available: <https://arxiv.org/abs/1905.07726>.
- [15] W. Lee, M. Kim, and D.-H. Cho, "Transmit power control using deep neural network for underlay device-to-device communication," *IEEE Wireless Commun. Lett.*, vol. 8, no. 1, pp. 141-144, Feb. 2019.
- [16] B. Zheng and R. Zhang, "Intelligent reflecting surface-enhanced OFDM: Channel estimation and reflection optimization," *IEEE Wireless Commun. Lett.*, Early Access.
- [17] D. Tse and P. Viswanath, *Fundamentals of wireless communication*. Cambridge university press, 2005.
- [18] S. Ioffe and C. Szegedy, "Batch normalization: Accelerating deep network training by reducing internal covariate shift," *Proceedings of The 32nd International Conference on Machine Learning*, pp. 448-456, 2015.
- [19] A. A. M. Saleh and R. Valenzuela, "A statistical model for indoor multipath propagation," *IEEE J. Sel. Areas Commun.*, vol. 5, no. 2, pp. 128-137, Feb. 1987.
- [20] M. Grant and S. Boyd, "CVX: Matlab software for disciplined convex programming, version 2.1," 2014.
- [21] G. Aceto, *et al.*, "MIMETIC: Mobile encrypted traffic classification using multimodal deep learning," *Computer Networks*, vol. 165, Dec. 2019.